ASIA-PACIFIC JOURNAL OF CHEMICAL ENGINEERING
Asia-Pac. J. Chem. Eng. 2010; **5**: 83–92
Published online 21 August 2009 in Wiley InterScience
(www.interscience.wiley.com) DOI:10.1002/apj.382

Curtin University of Technology

Special Theme Research Article

Membrane Reactor Modelling, Validation and Simulation for the WGS Reaction using Metal Doped Silica Membranes

*S. Battersby,[1] B. P. Ladewig,[2] M. Duke,[3] V. Rudolph[1] and J. C. Diniz da Costa[1]**

[1]*Films and Inorganic Membrane Laboratory, Division of Chemical Engineering, The University of Queensland, Brisbane, QLD 4072, Australia*
[2]*ARC Centre of Excellence for Functional Nanomaterials, Australian Institute of Bioengineering and Nanotechnology, The University of Queensland, Brisbane, QLD 4072, Australia*
[3]*Institute for Sustainability and Innovation Victoria University, Werribee Campus, Melbourne, VIC, 8001 Australia*

Received 23 October 2008; Revised 14 January 2009; Accepted 15 January 2009

ABSTRACT: In this work, a Matlab Simulink© model was developed to analyse and predict the performance of a metal doped silica membrane reactor for H_2 production via both the high and low temperature water gas shift reaction. An activated transport model for mixed gas separation with combined reaction was developed to model the effects within a membrane reactor unit. The membrane reactor was modelled as a number of perfectly mixed compartments containing a catalyst bed and a gas selective membrane. The combined model provided a good fit to experimentally measured results for higher conversions up to equilibrium, which is generally the case for industrial applications. Simulation results showed that H_2 separation and H_2 recovery improved with pressure, due to the H_2 concentration driving force across the membrane. For a single stage membrane reactor unit, a maximum conversion of 93% could be achieved with a H_2 recovery rate of 95%. In addition, the membrane reactor efficiency increased at higher temperatures and lower H_2O : CO feed ratios, allowing for CO conversion improvements by the membrane reactor. © 2009 Curtin University of Technology and John Wiley & Sons, Ltd.

KEYWORDS: membranes; water gas shift reaction; modelling; simulation; hydrogen

INTRODUCTION

There is currently a large world effort towards developing hydrogen power as the next generation of clean energy for both the transportation and the electricity sectors. The major advantage of this technology is possible when used in fuel cells, providing significantly higher efficiency compared to combustion technology.[1,2] It is likely that, at least in the intermediate term, hydrogen will be derived from fossil fuels, which currently account for 96% of all hydrogen produced in industry.[3] With current global reserves estimates ranging from 200 to 500 years, coal supplies are almost certain to surpass all other major fossil fuels.[4] As security of energy supply is a key concern for future economies, this means coal will long continue to be a major factor in global power supply.

In Australia the energy sector produces 60% of all CO_2 emissions with coal power generation accounting for 76% of all electricity produced.[5] However, as future energy scenarios become constrained by a decarbonised economy, the electricity sector will be forced to make large reductions in its emissions. For this to become a reality, technical solutions are necessary to address current limitations. One new major technology being developed is the Integrated Gasification Combined Cycle (IGCC) which uses a process called coal gasification (Eqn 1) to generate syngas (H_2 and CO) which is converted further in the water gas shift (WGS) reaction to produce optimal amounts of H_2 and CO_2 (reaction 2).

$$C_{(s)} + H_2O_{(g)} \rightarrow CO_{(g)} + H_{2(g)} \qquad \Delta H = 135.6 \text{ kJ/mol} \tag{1}$$

$$CO_{(g)} + H_2O_{(g)} \leftrightarrow CO_{2(g)} + H_{2(g)} \qquad \Delta H = -41.2 \text{ kJ/mol} \tag{2}$$

The WGS is an equilibrium limited, endothermic reaction, with higher temperatures resulting in accelerated reaction kinetics but lower equilibrium conversion. Conventional technologies (Fig. 1) utilise a high temperature shift (HTS) and low temperature shift (LTS) with high volumes of excess water to drive conversion. This process can reduce CO to around 1% by reacting

**Correspondence to*: J. C. Diniz da Costa, Films and Inorganic Membrane Laboratory, Division of Chemical Engineering, The University of Queensland, Brisbane, QLD 4072, Australia.
E-mail: j.dacosta@uq.edu.au

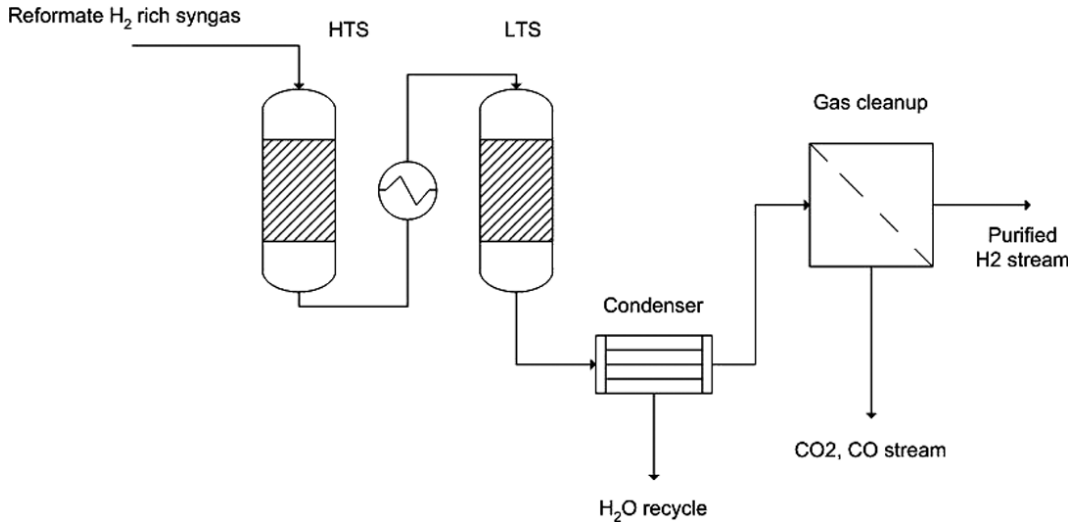

Figure 1. Schematic of a water gas shift, CO clean up stage.[10].

it with high steam contents to produce the maximum amount of H_2 possible.[6–9] However, downstream gas separation is needed to separate H_2 from the product stream, with possible sequestration of the CO_2.

An alternative strategy to optimise the WGS reaction is to employ a membrane reactor (MR), which integrates the reaction and product separation into a single unit, using a selective membrane, offering many benefits over conventional systems.[11–13] This is especially the case where *in-situ* product separation can enhance an equilibrium limited reaction, allowing the reactor to operate at more suitable temperatures.[14,15] In the WGS this has two main advantages; firstly by allowing operation at optimum temperatures a MR can provide improved reaction rates and reduce the need for excess water, improving plant efficiency. Secondly, by providing both reaction and product separation in one process step, a MR can potentially reduce the plant size and thus capital costs.[11,13,16]

With the development of inorganic membranes over the last 15 years, there has been a renewed interest in the field of MRs.[6,12–14,17,18] However, initial interest has mainly centred on simple dehydrogenation reactions, and improvement of WGS MR has only recently been investigated by a couple of groups.[6,7,19–21] Recent findings have outlined the potential of the WGS MR, investigating the effects of $H_2O:CO$ ratio[22] and feed pressure[23] on the enhancement of CO conversion. Combined with recent advances in hydrothermal stabilisation and development of highly selective silica membranes,[24,25] there is a real potential for development in this field of research.

Coupling a membrane and reactor as a single unit operation requires modelling the membrane transport mechanism together with the reactor's reaction mechanisms. In the case of the reactor, a simple yet practical model describing the reversible WGS reaction with an empirical power law rate expression was sufficient. This model is easier to implement and faster to compute, although it requires catalyst activation data and comparison with experimental results to validate the model. A number of empirical rate expressions and reaction orders are provided in Table 1. The rate expression is applied within the context of a reactor model, depending on the detailed physical conditions within the reactor at any point where the reaction occurs. The reactor model itself often uses simplifying assumptions to aid in design, eg plug flow, and isothermal and isobaric conditions.

For MRs, it has been found that non-ideal flow can have a large effect on the predicted conversion.[21] The dispersion model (DM) predicts non-ideal flow by modelling the dispersion of each component in both the axial and radial directions.[21,31–33] Alternatively a compartment model can be used, assuming perfect mixing within each compartment with exchange of mass, energy and entropy between compartments used to replicate non-ideal flow.[34] This provides a simplified method to approximate the effects of non-ideal flow on

Table 1. Empirical rate expression parameters ($r_{CO} = k_r P_{CO}^a P_{H2O}^b (1-\beta)$).

Catalyst	Reaction orders	ln k_o	E_A (kJ/mol)	References
$Cu/ZnO/Al_2O_3$	a = 1, b = 1	15.2	52.8	[26]
$Cu/ZnO/Al_2O_3$	a = 0, b = 1	12.6	47.4	[27]
		–	41.8	[28]
Pt/CeO	a = 1, b = 1	17.0	80.0	[9]
Fe_3O_4/Cr_2O_3	a = 1, b = 0	11.5	112	[29]
$Cu/Fe_3O_4/Cr_2O_3$		7	81	
Fe_3O_4/Cr_2O_3	a = 0.73, b = 0.55	–	110	[21,30]

DOI: 10.1002/apj

MR conversion. The assumption of isothermal operation in a reactor model depends on the extent and heats of reaction compared to the heat loss through the reactor walls. An adiabatic assumption (no heat loss) can also be used in comparison with isothermal operation, to analyse the maximum level of temperature gain possible for the given reaction. For pressure drop within the reactor, the Ergun equation is used.

In the case of gas mixtures, detailed modelling for gas separation and permeation through molecular sieving porous membranes is complex.[35] Several gas mixture models have been derived, including the Stefan-Maxwell approach,[36] and non-equilibrium[37] and finite mass exchange,[38] though each has its limitations for use with microporous membranes. An activated diffusion transport model was proposed by Barrer,[39] explaining the temperature dependency of pure gas transport through the membrane. Barrer's model addresses the transport of gas molecules through pores of sizes close to the dimension of the molecules. The model has been adapted to predict transport through the membrane of gas mixtures in the Henry's regime and validated for gas mixture separation.[40]

One potential issue that arises in the industrial application of a WGS MR is the use of high pressure (>15 bar). The adsorption of gases in silica derived membranes is generally at very low coverage at high temperatures; therefore Barrers' model is generally applicable within Henry's regime.[35,41,42] In this work, we propose a MR model for the water gas shift reaction operating under the conditions of Henry's adsorption regime and complying with Barrer's model. The model integrates chemical reaction rate, mass transport though the reactor and the membrane to simulate the performance of MR under various regimes of operation. The model was set up in Matlab Simulink© for simulation purposes. The model was also validated on the basis of experimental results.

MODEL DEVELOPMENT

Single stage design

The MR was modelled as a number of perfectly mixed compartments, containing a catalyst bed and a gas selective membrane. The model boundary for a single compartment reactor is shown in Fig. 2 below.

The defined variables are the following:

- Feed flow, composition and pressure (F_f, C_{f_j}, P_f)
- Sweep flow, composition and pressure (F_s, C_{s_j}, P_s)
- Reactor volume and temperature (V_{rxr}, T_{rxr})
- Reaction rate constant and equilibrium constant (k_r, K_{eq})
- Membrane permeance (P/l)

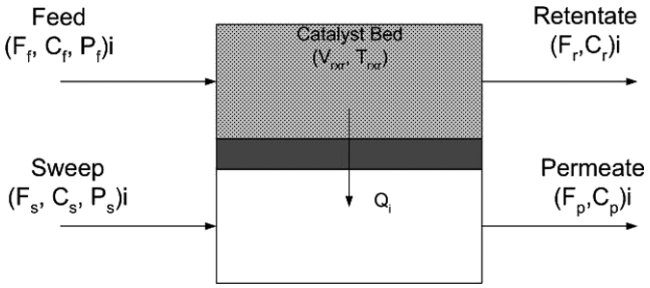

Figure 2. Model boundary for a single compartment MR unit.

The assumptions are the following:

- Perfectly mixed compartmental reactor
- Perfectly mixed permeate chamber (Permeation rate $\ll$ Gas to gas diffusion)
- Adiabatic reactor
- No side reactions
- Reactor pressure is kept constant and controlled by a back pressure valve
- No back permeation of species through the membrane
- Steady state operation.

Using these assumptions the mass balance over a single compartment can be described by the reaction rate equation:

$$\frac{dN_i}{dt} = \text{In} - \text{Out} + \text{generation} \tag{3}$$

which can be described in terms of the systems variables shown in Fig. 2:

$$\frac{V_{\text{rxr}} dN_i}{dt} = F_f C_{f\_j} - F_r C_{r\_j} - Q_i C_{q\_j} + V_{\text{rxr}} r_i \tag{4}$$

Assuming mass conservation is maintained within the system the outlet flow of a single compartment can be calculated as

$$F_\text{r} = F_\text{f} - F_\text{q} \tag{5}$$

where, the total permeate flowrate (F_q) is equal to the sum of all component permeation:

$$F_\text{q} = \Sigma Q\text{i} \tag{6}$$

Therefore, the final reactor mass balance equation can be derived by substituting Eqn 5 and 6 into Eqn 4, and rearranging for change in concentration:

$$\frac{dC_i}{dt} = \frac{F_\text{f} C_{\text{f\_j}} - (F_\text{r} - F_\text{q}) C_{\text{r\_i}} - Q_i}{V_{\text{rxr}}} + r_i \tag{7}$$

Assuming the reactor compartment is perfectly mixed, the reaction rate is defined by the gas concentrations at

DOI: 10.1002/apj

the outlet of the reactor. These concentrations are used in the reaction rate equation as follows:

$$r_i = k_r P^a_{r-\mathrm{CO}} P^b_{r-\mathrm{H2O}} (1-\beta) \tag{8}$$

where, the reactant partial pressures (P_i) can be calculated from the reactor concentrations (C_i) using the ideal gas law:

$$C_i = \frac{P_i}{RT_{\mathrm{rxr}}} \tag{9}$$

and the reversibility factor β is defined as

$$\beta = \frac{P_{\mathrm{CO2}} P_{\mathrm{H2}}}{P_{\mathrm{CO}} P_{\mathrm{H2O}} K_{eq}} \tag{10}$$

where, the equilibrium constant is defined by the thermodynamics of the chosen reaction.

This work assumes that the permeate chamber is perfectly mixed as the permeation rate $\ll$ bulk gas to gas diffusion.[16] The membrane's permeate flow rate (Q_i) is calculated as a factor of the permeance (P/l) (Table 3) and the partial pressure difference between the tube ($x_i P_f$) and shell ($y_i P_s$) side of the membrane for a gas component (i). This calculation is made for each species within the reaction chamber, giving the following equation:

$$Q_i = \left(\frac{P}{l}\right)_i (x_i P_{\mathrm{f}} - y_i P_{\mathrm{s}}) \times SA_{\mathrm{memb}} \tag{11}$$

Full MR design

The full MR is modelled as a series of connected reactor compartments with each compartment representing a length of the membrane tube (Fig. 3). The reaction in each compartment is modelled independently, with the outlet gas of each tank flowing on to the next tank along the membrane profile. In contrast, the permeate chamber is modelled as one distinct volume (perfectly mixed permeate chamber) and the permeate concentration is a factor of the total permeation from each single compartment.

Therefore, the total permeation flow rate (F_q) of the membrane tube then becomes

$$F_{\mathrm{q}} = \Sigma {Q_i}^1 + \Sigma {Q_i}^2 \ldots + \Sigma {Q_i}^{\mathrm{n}} \tag{12}$$

for each species (i) in compartment (n). The permeate concentration of each species (y_i) is then calculated as the fraction of the species i in the total permeation flow:

$$y_i = \frac{Q_i^1 + Q_i^2 .. + Q_i^n}{F_{\mathrm{q}}} \tag{13}$$

As each compartment is designed to be of the same size, the reactor volume and membrane area for each reactor compartment is defined as follows:

$$V_{\mathrm{rxr}} = \frac{\pi . r^2_{\mathrm{tube}} L_{\mathrm{tube}}}{n} \tag{14}$$

$$A_{\mathrm{memb}} = \frac{2\pi . r_{\mathrm{tube}} L_{\mathrm{tube}}}{n} \tag{15}$$

where, r_{tube} and L_{tube} are the tube radius (cm) and length (cm) for each compartment and n is the number of used compartments.

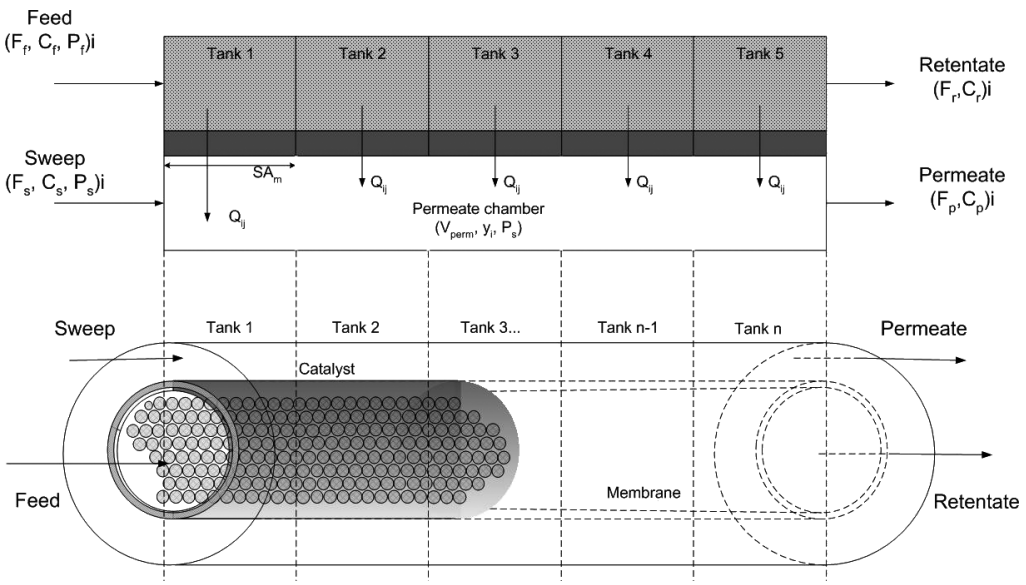

Figure 3. Schematic of full MR model compared to actual tubular MR unit.

DOI: 10.1002/apj

Pressure drop in a packed bed

Momentum loss in the catalyst bed is calculated using the well known Ergun Equation:

$$\frac{\Delta P}{L} = 150\frac{(1-\varepsilon)^2 \mu . u_s}{\varepsilon^3 d_p^2} + 1.75\frac{(1-\varepsilon)u_s^2 \rho}{\varepsilon^3 d_p^2} \qquad (16)$$

where, ΔP is the pressure drop (Pa) along the length of the reactor bed, L is the catalyst bed length (m), ε the bed porosity (−), μ the gas viscosity (Pa.s) and u_s the superficial velocity (m s^{-1}). Pressure drop is calculated at the end of each compartment, to determine the pressure drop across the reactor tube.

Adiabatic operation (no heat loss out of membrane tube)

The assumption of adiabatic operation is important to determine the level of heat gained in the reactor due to heat of reaction. This can be especially important for the modelling of scaled up MRs with industrial flow rates. The heat of reaction is calculated as a function of temperature:[13]

$$\Delta H_{\text{rxn}}(T) = \Delta H^{\circ}_{\text{rxn}}(T_R) + \Sigma x_i \Delta C_{p\_i} \times (T - T_R) \qquad (17)$$

where, ΔH°_{rxn} is −41 192 J mol^{-1} at 298 K; the heat term (Q_{rxn}) can then be calculated:

$$\Delta Q_{\text{rxn}} = \Delta H_{\text{rxn}} \times M_{\text{CO}}.X \qquad (18)$$

$$\Delta T = \frac{\Delta Q_{\text{rxn}}}{m.\Sigma(x_i C_{p\_i})} \qquad (19)$$

where, M is the molar flow rate of CO (mol s^{-1}), X is the conversion fraction of CO, m is the mass flow rate (g s^{-1}), x_i is the fraction of species i in the reactor and C_p is the specific heat of the species at the given temperature.

Table 2. Kinetics of tested catalysts.

Catalyst	ln k_o	E_A (kJ mol^{-1})	r^2
HTS cat (commercial Fe_3O_4/Cr_2O_3)	19.1	105.1	0.98
LTS cat (commercial $Cu/ZnO/Al_2O_3$)	12.9	50.7	0.97

MODEL VARIABLES

Catalyst activation energy

The activation energy of the high and low temperature WGS catalysts used in this work was determined experimentally in a packed bed reactor (PBR) prior to their use in the MR. Catalyst conversion was linearised and the linear regressions were fitted to calculate the activation energy and pre-exponential factors of the catalyst as listed in Table 2.

Membrane activated transport

The experimentally found permeance values of the membranes were used to determine the activated transport constants in the MS model. The permeance of the two membranes was linearised with temperature and the linear regression of the results (Fig. 4) was used to calculate the activation energy and pre-exponential factors of the membrane as listed in Table 3.

The linear regression fits provided high accuracy ($r^2 > 0.95$) with the exception of the CO_2 and N_2 measurements, which is attributed to the flow rate measurement variations at the lower permeance values ($<1 \times 10^{-11}$ mol m^{-2} s^{-1} Pa^{-1}). It was observed that the smaller molecules (H_2, He) showed high activation energies, while larger molecules (CO, CO_2, N_2) displayed negative activation energies. The latter

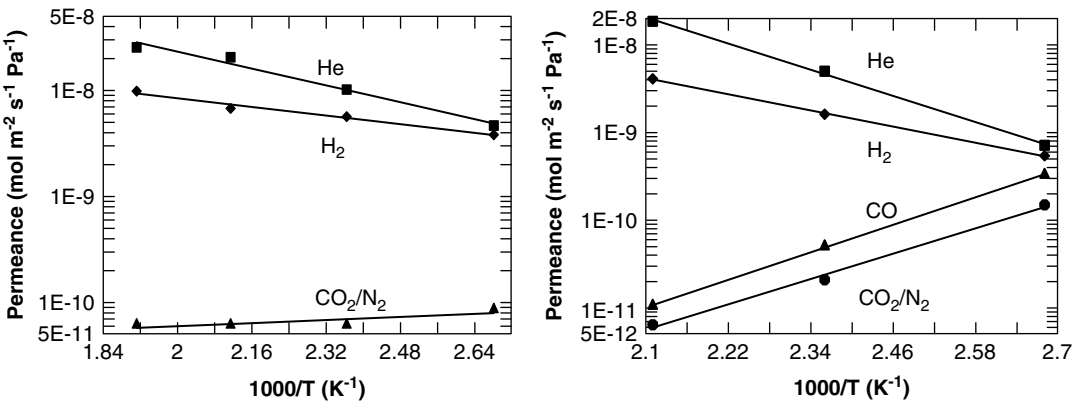

Figure 4. Tube membrane permeance linear regression fits for tubular cobalt silica membranes from (a)left: hydrothermal testing and (b)right: dry gas condition testing.

DOI: 10.1002/apj

Table 3. Activation energy (E_A kJ mol^{-1}), pre-exponential factor (ln Q) and r^2 values of the Arrhenius type linear regression fit for cobalt silica membranes permeation.

	Membrane 'A'			Membrane 'B'			
Membrane properties	He	H_2	CO_2 and N_2	He	H_2	CO	CO_2 and N_2
E_A (kJ/mol)	19.02	9.76	−6.36	20.69	12.7619	−21.75	−20.05
Ln (Q)	−13.00	−16.24	−25.27	−2.46	−5.156	−16.49	−16.31
r^2	0.98	0.97	0.92	0.99	0.99	0.99	0.91

is generally associated with the transport of larger molecules through pores of small sizes, where the potential of the pore exceeds the mobility potential of the larger gases.[43] The high activation energies for He and H_2 permeation indicated a high quality molecular sieving membrane.[41–43]

RESULTS AND DISCUSSIONS

Validation

The modelling of the PBR conversion with temperature for varying $H_2O:CO$ ratios is presented in Fig. 5. For the low temperature (Fig. 5a) and high temperature WGS (Fig. 5b), it is observed that the model provided a very good fit against the experimental CO conversions. While there were a couple of points for both temperatures with slightly higher deviation of around 8–10%, the majority of experimental points reflected the modeling results accurately with on a 2–3% difference in conversion.

The modelling of mixed gas separation is shown in Fig. 6. At high conversions, the concentrations of H_2 and CO_2 approach 50% in the MR reaction chamber, while CO reduces to values close to zero. At this condition, the model provides a good fit to gas permeation through the membranes. At low conversions, the concentration of CO is high (above 50%) and the model shows a deviation from 2 to 6.5%, equivalent to ~32.5% relative deviation. CO_2 simulation is quite consistent with the experimental results independent of the conversion rate. H_2 shows a reasonably good fit, although a deviation is observed at low conversion. These deviations may be attributed to the sorption effect of the high concentration species in the gas mixture (e.g. CO) at low conversions. The average pore size (and, hence, the percolation effect) influences the selectivity,[44] as demonstrated elsewhere for gas mixtures containing H_2.[45] This may explain that at low conversions and temperatures, the purity of H_2 is reduced due to a combined effect of CO adsorption and diffusivity, thereby causing pore blockage and reducing the percolation threshold for H_2 permeation. This is also reflected for the deviation in flow rates, as shown in Fig. 6b, where the model under predicts the

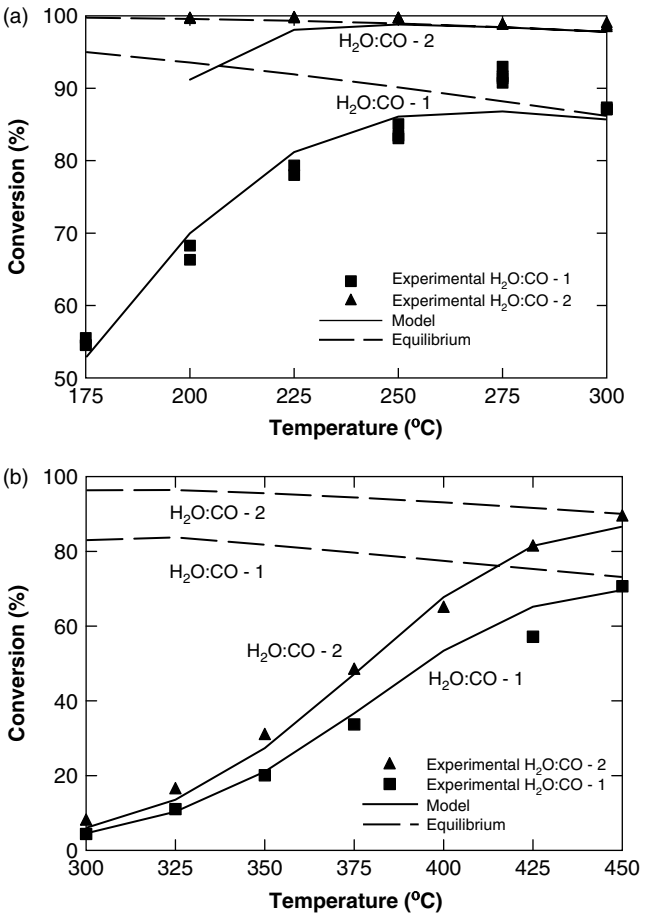

Figure 5. Model results compared to observed experimental conversion for the (a): LTS and (b): the HTS catalyst at varying $H_2O:CO$ feed ratios (1 or 2 H_2O) and temperatures.

H_2 flow rate at low conversions. Nevertheless, industrial processes are likely to operate at high conversions, where the model provides a good prediction of operating parameters and MR performance.

The MR model validation is a combination of the validated reaction and separation models above described. The membrane permeance values calculated during reaction are listed in Table 4.

The modelling of MR conversion compared to conventional PBR conversion is presented in Fig. 7. Model prediction below equilibrium conversion showed a good fit with experimental measurements, predicting the 5%

DOI: 10.1002/apj

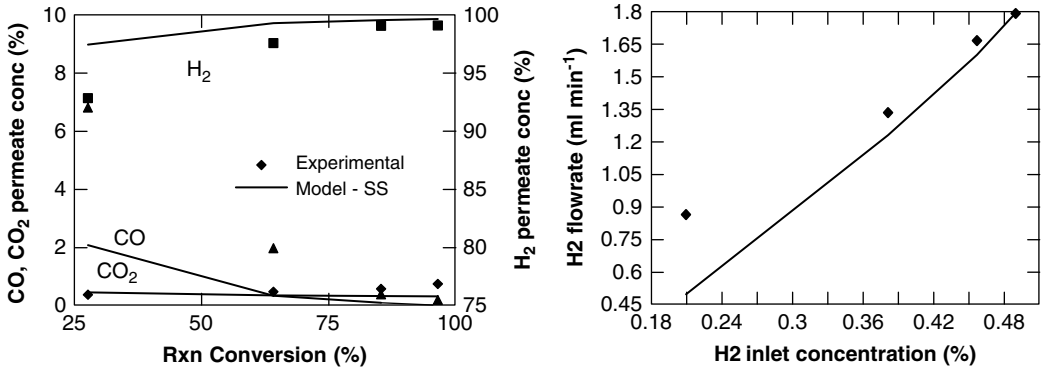

Figure 6. Steady and non steady state modelling of ternary gas mixture separation. (a)-left: normalised permeate concentrations (without sweep) and (b)-right: membrane H_2 flowrate (ml min^{-1}).

Table 4. Membrane permeance characteristics after hydrothermal treatment.

Gas type	Permeance (mol m^{-2} Pa^{-1} s^{-1}) @200 °C	Activation Energy (E_A)
H_2	4.8×10^{-10}	26.78
CO	5.1×10^{-11}	–
CO_2	2.20×10^{-11}	–

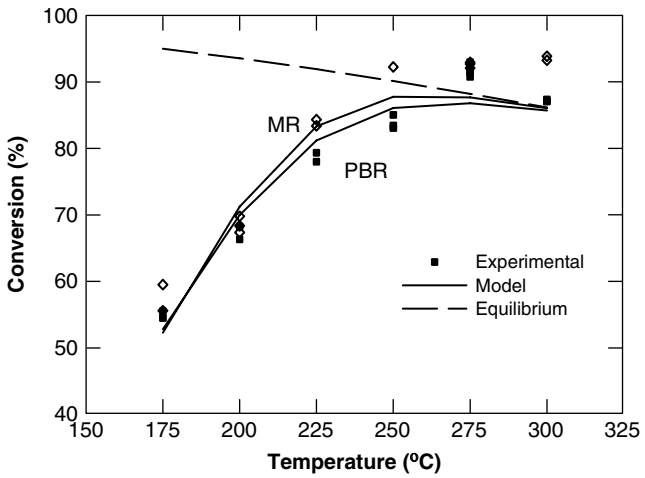

Figure 7. MR model results (lines) compared to experimentally found values (symbols) (H_2O ratio – 1, Inlet pressure – 4 bar).

enhancement between MR and PBR results. However, for the experimental conversion above equilibrium, the model showed large deviation, underestimating the effect of separation on conversion. The deviations in these results suggest that the equilibrium conversion is the limitation in the MR model in this work.

Separation modelling in the combined MR model provided a good fit to experimental results for both selectivity and permeation rate, as shown in Fig. 8. The deviations are generally observed at low conversion, where CO and H_2 slightly deviate from experimental results. Again, the deviations are attributed to the combined effect of CO adsorption and diffusion, which hinders the percolation effect of H_2 permeation.

Full scale MR simulation

Using the model parameters determined from the tube scale permeation and reaction testing, the full model was expanded to predict operation of the MR conversion and H_2 recovery based on the operational variables such as feed rate, pressure and permeate sweep rate. The membrane permeation and selectivity characteristics are from membrane 'b' (Table 3) while both high and low temperature catalysts have been analysed.

For optimisation of conversion, a high separation of H_2 from the syngas stream is necessary. Feed pressure and permeate sweep gas flow rate are the two main methods to enhance membrane flux, though both have their disadvantages including an energy penalty for compression costs and dilution of permeate stream due to sweep gas or vapour (i.e. steam). This means it is quite possible that a combination of the two factors is necessary for optimised separation. Fig. 9 shows the conversion enhancement of the WGS reaction for various sweep ratios (rate of sweep gas/rate of permeation) and inlet feed pressures. It can be seen that both pressure and sweep lead to enhanced conversion, with up to 20 bar pressure providing 4 and 11% enhancement for LTS and HTS respectively, while a sweep ratio of up to 7 provided 4% and 8% enhancement for LTS and HTS, respectively. The best enhancement however came from a combination of the two, with increased pressure and sweep providing 8% and 19% total conversion enhancement for LTS and HTS, respectively.

An important factor observed in Fig. 9 is the advantage of operating the MR at high temperature. The HTS

DOI: 10.1002/apj

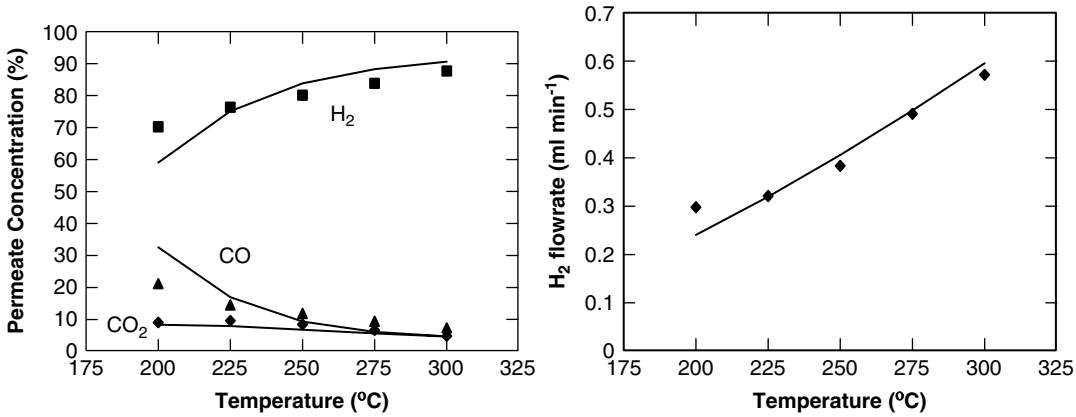

Figure 8. MR permeation model results (lines) compared to experimentally found permeate concentration and flux (symbols).

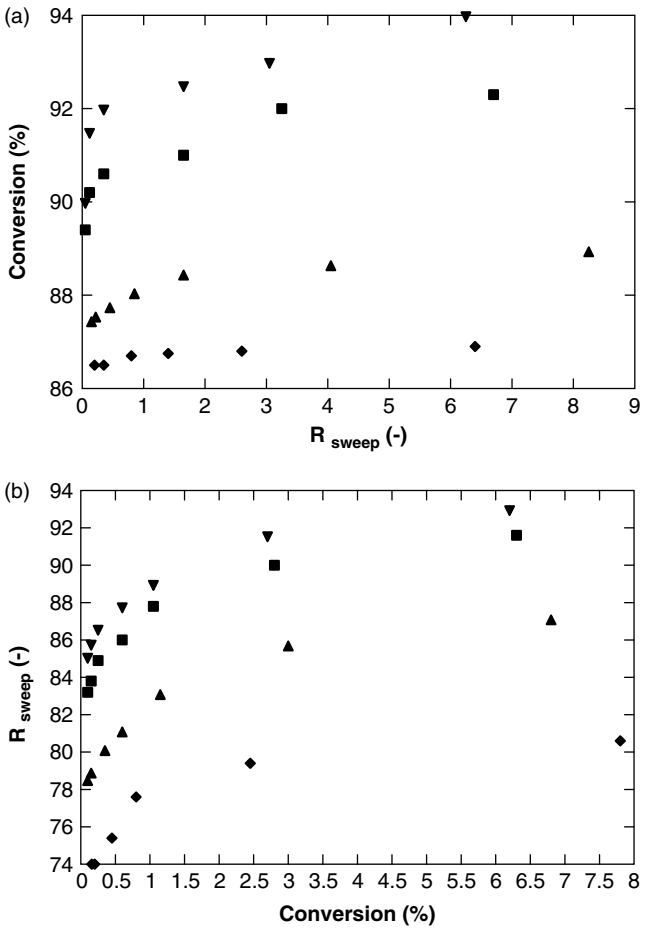

Figure 9. Model results for MR conversion *vs* sweep ratio (F_{sweep}/F_{perm}) for various inlet feed pressures for (a) LTS – 300 °C and (b) HTS – 450 °C. (♦ – 4bar, ▲ – 8bar, ■ – 15bar, ▼ – 20bar).

generally has lower conversion than the LTS due to equilibrium limits. However, the conversion enhancement is a factor of the H_2 diffusion through the membrane. In the case that conversion is already high then there is little improvement to be gained from separation. At HTS (450 °C), the conversion shifts as much as ~8%, thus providing greater improvement and resulting in similar conversion to the LTS.

Figure 10 models the effect of pressure and sweep on the H_2 recovery through the membrane. The recovery rate is the ratio of H_2 in the permeate stream over the total H_2 produced. The influence of pressure (or concentration driving force) on permeation is linear and directly proportional to permeance or flow rate in molecular sieving membranes. Depending on the operating temperature, changing the feed pressure from 4 to 15 bar, may increase H_2 recovery by as much as 50%, from 0.3 to 0.8 at 300 °C. However, the effect of pressure on H_2 diffusion through the membrane levels off around the 90% mark for high temperature (450 °C) and pressure at 15 bar, which is the permeation limitation due to the partial pressure driving force. An advantage of using sweep gas/vapour is the ability to improve an already high recovery level further (Fig. 10b). For instance, the addition of a sweep ratio of 1 for a 15 bar feed pressure, the H_2 recovery rate was improved from 92 to 95%, representing a valuable increase in H_2 removal.

A combined reaction and separation model was designed to effectively predict MR performance from the individually determined, temperature activated characteristics of both the catalyst and membrane. An empirical reaction rate expression was applied to CO conversion in the WGS reaction, with a 'perfectly mixed' single compartment used to model the effects of mass diffusion within the reaction tube. With the assumptions of adiabatic operation and consideration of pressure drop, conversion for both high and LTS was successfully modelled for different H_2O : CO ratios, pressures and temperatures. An activated diffusion transport model was used to predict gas permeation and separation across the membrane, derived from pure gas measurements and extended to simulate gas mixture separation.

DOI: 10.1002/apj

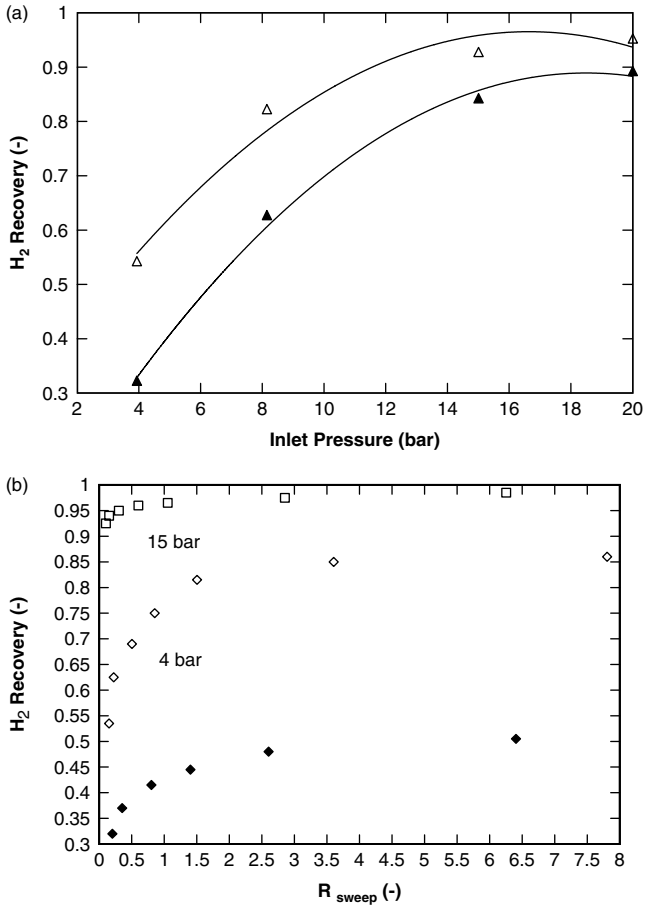

Figure 10. Model results for H_2 recovery rate *vs* (a) inlet pressure and (b) and sweep ratio for HTS (open symbols) and LTS (closed symbols).

The application of the validated MR model was used to analyse the effects of operational variables on the performance of the MR. This included consideration of temperature, pressure, sweep rate and inlet feed rate. In the optimisation of H_2 recovery, a balance of pressure and sweep gas was found to provide the best advantage with up to 95% recovery achieved at 15 bar pressure and sweep ratio of 1. High inlet pressure was used to drive separation through increased H_2 partial pressure on the feed side of the membrane. However, as the H_2 recovery rate increased, the concentration of H_2 in the reactor chamber decreased, thus limiting the driving force for gas permeation. To provide extra H_2 recovery, the use a sweep gas/vapour in this situation was effective, maintaining optimised separation by reducing the partial pressure on the permeate side of the membrane.

CONCLUSIONS

An activated transport model for mixed gas separation with combined reaction was developed to model the effects within an MR unit. The use of an empirical reaction rate expression with a 'perfectly mixed' single compartment model was applied to predict conversion through the catalyst bed, while an activated transport model derived from single gas permeance values was applied to predict mixed gas separation through the membrane. The combined model provided a good fit to experimentally measured results, showing good validation with permeate flow rate and concentration for higher conversions, and good validation with reactor conversion up to equilibrium. The deviation between experimental and simulation results occurred at low CO conversions and low temperatures. These were mainly attributed to CO adsorption, which affected the H_2 percolation threshold, thus affecting H_2 flow and purity. However, industrial applications are likely to be operating at high conversions and temperature, within the high accuracy range of the MR model.

The application of the validated MR model was used to analyse the effects of operational variables on the performance of the system. This included consideration of temperature, pressure, sweep rate and inlet feed rate. Use of pressure provided the greatest improvement in H_2 separation with an increase of 50% recovery possible from 4-15 bar feed pressure. In comparison the advantage of using sweep gas/vapour is the ability to improve an already high recovery level further. While both factors allowed feasible operation of the membrane, to maintain the H_2 driving force across the membrane a balance of these two factors is necessary. For a single stage MR unit, a maximum conversion of 93% conversion could be achieved with a H_2 recovery rate of 95%. It was observed that the best performance of the MR was achieved at lower feed $H_2O:CO$ ratios and higher temperatures, as the lower equilibrium limit allowed greater enhancement of conversion.

Acknowledgements

Scott Battersby acknowledges scholarship support from the CCSD – Cooperative Research Centre (CRC) for Coal in Sustainable Development. The authors acknowledge financial research funding support via the Innovation Funds given by the Queensland Government (Australia), and by the Centre for Low Emission Technology (www.clet.net).

REFERENCES

[1] D.J. Holt. *Hydrogen and Its Future as a Transportation Fuel*, SAE International: Warrendale, **2003**.
[2] C.A. McAuliffe. *Hydrogen and Energy*, Gulf Publishers Co., Book Division: Houston, **1980**.
[3] B.C.R. Ewan, R.W.K. Allen. *Int. J. Hydrogen Energy,* **2005;** *30*, 809–819, DOI: 10.1016/j.ijhydene.2005.02.003.
[4] B. McLellan, E. Shoko, A.L. Dicks, J.C.D. da Costa. *Int. J. Hydrogen Energy,* **2005;** *30*, 669–679.

[5] M. Ferguson. *Energy in Australia*, Australian Department of Resources Energy and Tourism, **2008**.
[6] A. Basile, A. Criscuoli, F. Santella, E. Drioli. *Gas Sep. Purif.,* **1996;** *10*, 243–254.
[7] A. Criscuoli, A. Basile, E. Drioli. *Catal. Today,* **2000;** *56*, 53–64.
[8] E. Xue, M. Okeeffe, J.R.H. Ross. *Catal. Today,* **1996;** *30*, 107–118.
[9] C. Wheeler, A. Jhalani, E.J. Klein, S. Tummala, L.D. Schmidt. *J. Catal.,* **2004;** *223*, 191–199.
[10] M.V. Twigg. *Catalyst Handbook*, John Wiley & Sons: New York, **1996**.
[11] M. Bracht, P.T. Alderliesten, R. Kloster, R. Pruschek, G. Haupt, E. Xue, J.R.H. Ross, M.K. Koukou, N. Papayannakos. *Energ. Convers. Manage.,* **1997;** *38*, S159–S164.
[12] A.G. Dixon. *Int. J. Chem. React. Eng.,* **2003;** *1*, 1–R6.
[13] A. Julbe, D. Farrusseng, C. Guizard. *J. Membr. Sci.,* **2001;** *181*, 3–20.
[14] J.N. Armor. *J. Membr. Sci.,* **1998;** *147*, 217–233.
[15] N. Itoh, T.H. Wu. *J. Membr. Sci.,* **1997;** *124*, 213–222.
[16] A. Criscuoli, A. Basile, E. Drioli, O. Loiacono. *J. Membr. Sci.,* **2001;** *181*, 21–27.
[17] G. Saracco, H.W.J.P. Neomagus, G.F. Versteeg, W.P.M. van Swaaij. High-temperature membrane reactors: potential and problems, *Proceedings of 15th International Symposium on Chemical Reaction Engineering*, Newport, **1998**.
[18] J.G. Sanchez Marcano and T.T. Tsotsis. *Catalytic Membranes and Membrane Reactors*, Wiley-VCH: Weinheim **2002;** pp.170–200.
[19] G. Barbieri, A. Brunetti, T. Granato, P. Bernardo, E. Drioli. *Ind. Eng. Chem. Res.,* **2005;** *44*, 7676–7683.
[20] Y.C.V. Delft, L.A. Correia, J.P. Overbeek, D.F. Meyer, P.P.A.C. Pex, J.W. Dijkstra, D. Jansen. Hydrogen membrane reactor for industrial hydrogen production and power generation, *Proceedings of 6th International Conference on Process Intensification*, Delfth, The Netherlands, **2005**.
[21] M.K. Koukou, N. Papayannakos, N.C. Markatos. *Chem. Eng. J.,* **2001;** *83*, 95–105.
[22] S. Giessler, L. Jordan, J.C.D. da Costa, G.Q. Lu. *Sep. Purif. Technol.,* **2003;** *32*, 255–264.
[23] A. Brunetti, G. Barbieri, E. Drioli, K.H. Lee, B. Sea, D.W. Lee. *Chem. Eng. Process.,* **2007;** *46*, 119–126.
[24] M.C. Duke, J.C.D. da Costa, G.Q. Lu, M. Petch, P. Gray. *J. Membr. Sci.,* **2004;** *241*, 325–333.
[25] M. Kanezashi, M. Asaeda. *J. Membr. Sci.,* **2006;** *271*, 86–93.
[26] R.L. Keiski, O. Desponds, Y.F. Chang, G.A. Somorjai. *Appl. Catal., A,* **1993;** *101*, 317–338.
[27] Y. Choi, H.G. Stenger. *J. Power Sources,* **2003;** *124*, 432–439.
[28] M.J.L. Gines, N. Amadeo, M. Laborde, C.R. Apesteguia. *Appl. Catal. A: Gen.,* **1995;** *131*, 283–296.
[29] C. Rhodes, B.P. Williams, F. King, G.J. Hutchings. *Catal. Commun.,* **2002;** *3*, 381–384.
[30] R.L. Keiski, T. Salmi, V.J. Pohjola. *Chem. Eng. J. Bioch. Eng.,* **1992;** *48*, 17–29.
[31] A. Basile, G. Chiappetta, S. Tosti, V. Violante. *Sep. Purif. Technol.,* **2001;** *25*, 549–571.
[32] M.K. Koukou, N. Papayannakos, N.C. Markatos, M. Bracht, H.M. Van Veen, A. Roskam. *J. Membr. Sci.,* **1999;** *155*, 241–259.
[33] M. Kumar, S. Agarwal, G. Pugazhenthi, A. Shukla, A. Kumar. *J. Membr. Sci.,* **2006;** *275*, 110–118.
[34] H.S. Fogler. *Elements of Chemical Reaction Engineering*, Prentice: Upper Saddle River, **2006**.
[35] A.J. Burggraaf. *J. Membr. Sci.,* **1999;** *155*, 45–65.
[36] R. Krishna, J.A. Wesselingh. *Chem. Eng. Sci.,* **1997;** *52*, 861–911.
[37] S.T. Hwang. *AIChE J.,* **2004;** *50*, 862–870.
[38] D.D. Do, K. Wang. *AIChE J.,* **1998;** *44*, 68–82.
[39] R.M. Barrer. *J. Chem. Soc., Faraday Trans.,* **1990;** *86*, 1123–1130.
[40] M.C. Duke, J.C.D. da Costa, G.Q. Lu, P.G. Gray. *AIChE J.,* **2006;** *52*, 1729–1735.
[41] R.S.A. De Lange, J.H.A. Hekkink, K. Keizer, A.J. Burggraaf. *J. Porous Mater.,* **1995;** *2*, 141–149.
[42] J.C. Diniz da Costa, G.Q. Lu, V. Rudolph, Y.S. Lin. *J. Membr. Sci.,* **2002;** *198*, 9–21.
[43] R.M. de Vos, H. Verweij. *Science,* **1998;** *279*, 1710–1711.
[44] F. Chen, R. Mourhatch, T.T. Tsotsis, M. Sahimi. *J. Memb. Sci.,* **2008;** *315*, 48.
[45] S. Gopalakrishnan, J.C. Diniz da Costa. *J. Memb. Sci.,* **2008;** *323*, 144–147.